

# Domain enhanced interlayer coupling in ferroelectric/paraelectric superlattices

V. A. Stephanovich,<sup>1</sup> I. A. Luk'yanchuk,<sup>2,3</sup> and M. G. Karkut<sup>2</sup>

<sup>1</sup>University of Opole, Institute of Mathematics and Informatics, Opole, 45-052, Poland

<sup>2</sup>University of Picardie Jules Verne, Laboratory of Condensed Matter Physics, Amiens, 80039, France

<sup>3</sup>L. D. Landau Institute for Theoretical Physics, RAS, 117940 GSP-1, Moscow, Russia

(Dated: November 5, 2018)

We investigate the ferroelectric phase transition and domain formation in a periodic superlattice consisting of alternate ferroelectric (FE) and paraelectric (PE) layers of nanometric thickness. We find that the polarization domains formed in the different FE layers can interact with each other via the PE layers. By coupling the electrostatic equations with those obtained by minimizing the Ginzburg-Landau functional we calculate the critical temperature of transition  $T_c$  as a function of the FE/PE superlattice wavelength  $\Lambda$  and quantitatively explain the recent experimental observation of a thickness dependence of the ferroelectric transition temperature in  $\text{KTaO}_3/\text{KNbO}_3$  strained-layer superlattices.

PACS numbers: 77.55.+f, 77.80.Dj, 77.80.Bh

In the past decade refinements in deposition techniques have made it possible to fabricate nanoscale size oxide ferroelectric superlattices with the objective to merge and optimize the technological properties of the constitutive materials [1, 2, 3]. In designing such artificial structures an understanding of the physics of underlying processes is essential to determine whether the resulting characteristics are provided simply by the superposition of the bulk properties of the constituents or whether the interface and finite-size effects play a predominant role.

Two competing types of phenomena that arise at the ferroelectric interface can affect the properties of the superlattices. The strain field, generated by the mechanical mismatch between the superlattice layers, influences the polarization orientation and generally increases the ferroelectric transition temperature  $T_c$  [4]. In contrast, the electric depolarization field, produced by interfacial surface charges is unfavorable to the formation of the ferroelectric phase [5]. In fact, in cubic perovskite-like ferroelectrics the situation can be even more complex due the formation of both  $180^\circ$  ferroelectric [6] and  $90^\circ$  ferroelastic [4, 7, 8] domains. Although the properties of ferroelectric superlattices can be governed by domain structure, no systematic study of this effect has to our knowledge been performed.

In the present paper, we address the question of ferroelectric domain formation in a periodic superlattice structure consisting of alternate ferroelectric (FE) and paraelectric (PE) layers of equal nanometric width  $2a_f = 2a_p$ . So as to avoid the complications of the effect of  $90^\circ$  ferroelastic domains we assume that the ferroelectric layers have either natural or strain-induced c-oriented uniaxial symmetry. We will show that the domain patterns formed in the different FE layers interact with each other across the PE layers via the spatially inhomogeneous depolarization electric field emerging from the domains of the neighboring FE layers as shown in Fig. 1. This proximity type effect is dependent critically on the thickness

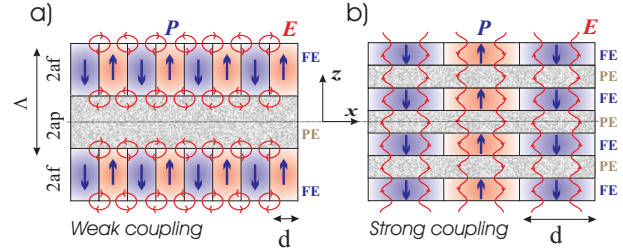


FIG. 1: Domains and depolarization field in weak (a) and strong (b) coupled ferroelectric layers in FE/PE superlattice close to  $T_c$

of the PE layers. Our interest has also been motivated by a recent experimental study of FE/PE superlattices of  $\text{KTaO}_3/\text{KNbO}_3$  [9] in which, as the superlattice wavelength  $\Lambda = 2a_f + 2a_p$  decreases, the ferroelectric transition temperature  $T_c$  first decreases and then saturates below a certain layer thickness. Such dependence was reproduced using molecular dynamics simulations [10] but the role of depolarizing effects was not elucidated. Attributing the observed behavior of critical temperature to the domain coupling in FE layers across the PE layers, we calculate the dependence  $T_c(\Lambda)$  and show that this dependence correctly reproduces the experimental behavior.

The physics underlying the domain formation and interaction is as follows. It is well known that a ferroelectric slab or thin film of thickness  $2a_f$  will separate into domains. This is to reduce the energy of the depolarization field produced by the space and surface charges with charge density  $\rho(r) = \text{div}\mathbf{P}$  that are provided by the discontinuity and non-uniformity of the polarization close to the crystal surface. In the Kittel approximation [11, 12, 13], applicable at  $T \ll T_c$ , the polarization inside a domain is assumed to be uniform and almost equal to its equilibrium value  $P_0$ . Thus the depolarization field is

proportional to the polarization discontinuity  $E_\sigma \sim 4\pi P_0$  and is confined to a thin layer of penetration length  $\delta$  that is roughly proportional to the domain size  $d$ . The equilibrium domain structure is the result of a balance between two competing energies (calculated per unit surface of crystal): the depolarization energy  $F_\sigma \sim \delta E_\sigma^2 \sim dP_0^2$  and the energy due to polarization gradients inside the domain walls  $F_w \sim a_f \Delta P_0^2 n \sim \Delta P_0^2 (a_f/d)$  where the length scale parameter  $\Delta$  is called a "domain wall width" and  $n \sim 1/d$  is the wall concentration. Minimization of  $F_\sigma + F_w$  gives the famous Kittel formula:  $d \sim \sqrt{\Delta a_f}$  [11, 12].

The coupling between FE layers in a FE/PE superlattice is caused by the depolarization field emerging from the domain structure of the FE layers. This interaction is exponentially small and the FE layers are almost independent if the distance between them  $2a_p$  is larger than the penetration length  $\delta$ . Taking into account that  $\delta$  scales as  $a_f^{1/2}$ , we determine that for an equally layered superlattice with  $2a_p = 2a_f = \Lambda/2$  this weak coupling regime is realized for long wavelength  $\Lambda$ . In the opposite limit of short  $\Lambda$ , the depolarization field penetrates the PE layers and so couples the domains in the neighboring ferroelectric layers. In this strongly coupled regime the domain size exceeds the superlattice wavelength and the superlattice behaves effectively as a uniform "composite" ferroelectric.

Close to the ferroelectric transition the polarization varies gradually inside domains, the charge and depolarization field penetrate FE layers so that the Kittel approximation is no longer applicable. In order to determine the domain structure parameters in FE/PE superlattices close to  $T_c$  and also the domain-formation-induced reduction of  $T_c$  with respect to the bare  $T_{c0}$  of a bulk sample in which the depolarization field is screened by the short circuited electrodes, we generalize the analogous calculations [14] for a thick ferroelectric plate. We start from the complete system of electrostatic equations:

$$\text{div}(\mathbf{E} + 4\pi\mathbf{P}) = 0, \quad \text{rot } \mathbf{E} = 0, \quad (1)$$

in which the polarization is related to the electric field by the constitutive relation  $\mathbf{P} = \mathbf{P}(\mathbf{E})$ . This is to be determined from both the nonlinear Ginzburg-Landau equation for the  $z$ -component of the spontaneous polarization in the uniaxial ferroelectric layers  $P = P_z^{(f)}$ :

$$tP + P_0^{-2}P^3 - \xi_0^2 \nabla^2 P = \frac{\varepsilon_{\parallel}}{4\pi} E_z^{(f)}, \quad (2)$$

(here  $t = T/T_{c0} - 1$ ,  $\nabla^2 = \partial_z^2 + \partial_x^2$ ) and by the linear relations for the two polarization components  $P_{x,z}^{(p)}$  in the PE-layers as well as for the transversal component  $P_x^{(f)}$  in the FE-layers:

$$P_x^{(f)} = \frac{\varepsilon_{\perp} - 1}{4\pi} E_x^{(f)}, \quad P_{x,z}^{(p)} = \frac{\varepsilon_p - 1}{4\pi} E_{x,z}^{(p)}. \quad (3)$$

The susceptibility  $\varepsilon_p$  of the PE-layers in (3) is assumed to be isotropic. The dimensionless parameter  $\varepsilon_{\parallel} \gg 1$  in (2) is expressed via the Curie constant as  $\varepsilon_{\parallel} = C/T_{c0}$ . The length  $\xi_0 \simeq 6\text{\AA}$  is estimated as the domain wall half-width at low temperatures, i.e. well below the phase transition. Hereafter we shall scale all the lengths in units of  $\xi_0$ .

The formulation of the problem is completed by the electrostatic boundary conditions at the PE/FE interfaces:

$$E_z^{(f)} - E_z^{(p)} = -4\pi(P_z^{(f)} - P_z^{(p)}), \quad E_x^{(f)} = E_x^{(p)} \quad (4)$$

and by the interface condition for the spontaneous polarization:

$$\partial_z P = \lambda P, \quad (5)$$

where  $\lambda$  is the extrapolation length [1, 15] that reflects the properties of the interface.

Close to the ferroelectric transition Eq.(2) can be linearized by neglecting the term  $P_0^{-2}P^3$ . The dimensionless transition temperature  $t_c$ , where the instability to the formation of a multidomain structure first appears, can be found as the highest eigenvalue of the linearized system of equations (1), (2) and (3) with the appropriate boundary conditions (4) and (5).

In terms of the electrostatic potential  $\varphi^{(f,p)}$ :  $E_{z,x}^{(f,p)} = -\partial_{z,x}\varphi^{(f,p)}$ , the full set of linearized equations takes the form:

*PE-layers:*

$$(\partial_z^2 + \partial_x^2)\varphi^{(p)} = 0. \quad (6)$$

*FE-layers:*

$$4\pi\varepsilon_{\parallel}^{-1}(t - \nabla^2)P = -\partial_z\varphi^{(f)}, \quad (7)$$

$$(\partial_z^2 + \varepsilon_{\perp}\partial_x^2)\varphi^{(f)} = 4\pi\partial_z P. \quad (8)$$

*PE/FE interface:*

$$\partial_z\varphi^{(f)} - \varepsilon_p\partial_z\varphi^{(p)} = 4\pi P, \quad (9)$$

$$\varphi^{(f)} = \varphi^{(p)}, \quad \partial_z P = \lambda P. \quad (10)$$

The eigenfunctions of the system of elliptic equations (6), (7) and (8) are the linear superposition of the harmonic functions which we write as:

*For the upper (lower) FE-layer* (see Fig. 1)

$$P = \left[ P_1 \frac{\cosh k_1 \left( z \mp \frac{\Lambda}{2} \right)}{\cosh k_1 a_f} + P_2 \frac{\cosh k_2 \left( z \mp \frac{\Lambda}{2} \right)}{\cosh k_2 a_f} \right] \cos qx, \quad (11)$$

$$\varphi^{(f)} = \left[ \varphi_1 \frac{\sinh k_1 \left( z \mp \frac{\Lambda}{2} \right)}{\sinh k_1 a_f} + \varphi_2 \frac{\sinh k_2 \left( z \mp \frac{\Lambda}{2} \right)}{\sinh k_2 a_f} \right] \cos qx.$$

*For the central PE-layer*

$$\varphi^{(p)} = -(\varphi_1 + \varphi_2) \frac{\sinh qz}{\sinh qa_p} \cos qx. \quad (12)$$

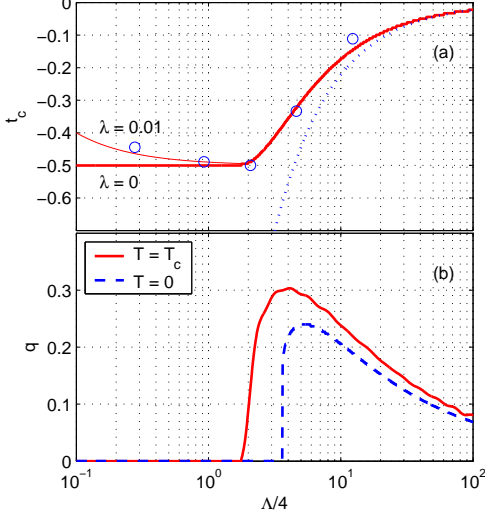


FIG. 2: Critical temperature  $t_c = T_c/T_{c0} - 1$  (a) and domain structure wave vector  $q = \pi/d$  at  $T = 0$  and  $T = T_c$  (b) as a function of superlattice wavelength  $\Lambda = 2a_f + 2a_p$ . Dotted line shows the asymptote (21). Circles show the experimental data for  $\text{KTaO}_3/\text{KNbO}_3$  superlattice [9]. The best fit parameters  $\varepsilon_{\parallel} = 400$ ,  $\varepsilon_{\perp} = 500$ ,  $\varepsilon_p = 800$ ,  $\lambda = 0$  and  $\lambda = 0.01$  have been used. The length is scaled in units of  $\xi_0 \simeq 6\text{\AA}$

In (12) the boundary conditions (10) were assumed. The periodicity of the oscillating factor  $\cos qx$  reflects the formation of a regular domain structure in the  $x$ -direction with domain size  $d = \pi/q$ . The solutions (11) and (12) can be periodically continued in the  $z$ -direction so as to follow the regular FE/PE superlattice structure.

The parameters  $P_{1,2}$ ,  $\varphi_{1,2}$  and  $k_{1,2}$  are found by substitution of (11) and (12) back into (6),(7),(8),(9) and (10). This permits us to find two characteristic equa-

tions defining the eigentemperature  $t = t(q)$ .

Substitution of solutions (11) into Eqs. (7) and (8) produces a homogeneous system of linear equations for  $\varphi_{1,2}$  and  $P_{1,2}$ :

$$\begin{aligned} 4\pi\varepsilon_{\parallel}^{-1} (t - k_{1,2}^2 + q^2) P_{1,2} + k_{1,2} \coth(k_{1,2}a_f) \varphi_{1,2} &= 0, \\ 4\pi k_{1,2} P_{1,2} - (k_{1,2}^2 - \varepsilon_{\perp}q^2) \coth(k_{1,2}a_f) \varphi_{1,2} &= 0, \end{aligned} \quad (13)$$

that are compatible if the characteristic equation

$$(k_{1,2}^2 - \varepsilon_{\perp}q^2) (t - k_{1,2}^2 + q^2) + \varepsilon_{\parallel}k_{1,2}^2 = 0 \quad (14)$$

is satisfied.

Now, to obtain the  $t(q)$  dependence we need one more equation relating  $t$ ,  $k$ , and  $q$ . This equation follows from the boundary conditions. Condition (9) gives the following relation between  $\varphi_{1,2}$  and  $P_{1,2}$ :

$$Q_1 \coth k_1 a_f \varphi_1 + Q_2 \coth k_2 a_f \varphi_2 = 4\pi (P_1 + P_2), \quad (15)$$

with  $Q_{1,2} = k_{1,2} + \varepsilon_p q \coth qa_p \tanh k_{1,2} a_f$ , while condition (5) gives:

$$P_1 (k_1 \tanh k_1 a_f - \lambda) + P_2 (k_2 \tanh k_2 a_f - \lambda) = 0. \quad (16)$$

Using (13) we can express  $\varphi_{1,2}$  as a function of  $P_{1,2}$ :

$$\varphi_{1,2} = P_{1,2} \frac{4\pi k_{1,2}}{k_{1,2}^2 - \varepsilon_{\perp}q^2} \tanh k_{1,2} a_f. \quad (17)$$

Substitution of (17) into (15) yields:

$$P_1 \left[ \frac{k_1 Q_1}{k_1^2 - \varepsilon_{\perp}q^2} - 1 \right] + P_2 \left[ \frac{k_2 Q_2}{k_2^2 - \varepsilon_{\perp}q^2} - 1 \right] = 0. \quad (18)$$

The compatibility criterion of equations (18) and (16) gives the second characteristic equation

$$\frac{k_1^2 - \varepsilon_{\perp}q^2}{k_2^2 - \varepsilon_{\perp}q^2} \frac{\varepsilon_{\perp}q \tanh qa_p + \varepsilon_p k_2 \tanh k_2 a_f}{\varepsilon_{\perp}q \tanh qa_p + \varepsilon_p k_1 \tanh k_1 a_f} = \frac{k_2 \tanh k_2 a_f - \lambda}{k_1 \tanh k_1 a_f - \lambda}. \quad (19)$$

The eigentemperature  $t(q)$ , transition temperature  $t_c = \max_q t(q)$  and the corresponding domain structure wave vector  $q_c$  are found from equations (14) and (19) after eliminating the variables  $k_{1,2}$ . The numerically obtained results for  $t_c$  and  $q_c$  as a function of superlattice wavelength  $\Lambda$  are plotted in Fig. 2 together with the experimental results of Ref. [9] on  $t_c(\Lambda)$  in  $\text{KTaO}_3/\text{KNbO}_3$  superlattice. The parameters we used to achieve this remarkably good fit were:  $\varepsilon_{\parallel} = 400$ ,  $\varepsilon_{\perp} = 500$ ,  $\varepsilon_p = 800$ ,  $\lambda = 0$  and  $\lambda = 0.01$ .

Two regimes that correspond to the above described

weak and strong coupling limits are clearly seen in Fig. 2. With decreasing  $\Lambda$  the domain size decreases, goes through a minimum and then diverges.

In the *weak coupling regime* ( $\Lambda > 20$ ) the domain size is smaller than the superlattice wavelength and the depolarization field is confined essentially at the FE/PE interfaces. Considering each FE layer as an independent thick film embedded in the PE media and using the substitution  $p_2 = ik_2$  (so that  $k_2 \tanh k_2 a_f = -p_2 \tan p_2 a_f$ ) we can simplify Eq. (19) to the form:

$$\varepsilon_{\perp}q \tanh qa_p - \varepsilon_p p_2 \tan p_2 a_f \approx 0 \quad (20)$$

that was first worked out in [14]. Using Eqs. (14) and (20) the behavior of  $p_2$ ,  $q_c^2$  and  $t_c$  reduces to:

$$p_2 \approx \frac{\pi}{2a_f}, \quad q_c^2 \approx \sqrt{\frac{\varepsilon_{\parallel}}{\varepsilon_{\perp}}} \frac{\pi}{2a_f}, \quad t_c \approx -\sqrt{\frac{\varepsilon_{\parallel}}{\varepsilon_{\perp}}} \frac{\pi}{a_f}. \quad (21)$$

The critical temperature  $t_c$  is inversely proportional to  $a_f$ , exactly as was found numerically in [16].

In the *strong coupling regime*, below a certain critical thickness ( $\Lambda < 5$ ) the domain structure abruptly disappears. The transition temperature of single-domain FE/PE superlattice is calculated from (14) and (19) by assuming  $q = 0$ :

$$t_c \approx -\frac{\varepsilon_{\parallel}}{\varepsilon_p} + \frac{\lambda}{a_f}, \quad (22)$$

or, equivalently, from the Landau energy of a periodic FE/PE structure with no depolarizing surface charges at the FE/PE interfaces. The FE/PE superlattice behaves as a uniform composite ferroelectric with a critical temperature (22), greater than that of the individual FE layers (21). The positive surface  $\lambda$ -term tends to increase  $t_c$  and this is possibly the reason for the slight increase of the transition temperature in the  $\text{KTaO}_3/\text{KNbO}_3$  superlattice at very small  $\Lambda$  [9], as shown in Fig. 2. Note that although the ferroelectric domains can exist in the strong coupling regime, their size is larger than the superlattice wavelength  $\Lambda$  and is defined by the global depolarization field of the sample.

To estimate the temperature evolution of the domain structure we express its energy at  $T = 0$  (i.e. at  $t = -1$ ) in the Kittel approximation, assuming an abrupt structure of the domain wall and a flat polarization profile inside the domains. The calculations are practically the same as those performed for the domain structure of the uniaxial ferroelectric film surrounded by paraelectric passive layers and embedded in a short circuited capacitor [6]. The free energy is the sum of the domain walls energy and the electrostatic contributions:

$$\pi F/P_0^2 = 2a_f \Delta q + \frac{32}{q} \sum_{n=1,3,\dots} \frac{1}{n^3} \frac{1}{g_n(q)}, \quad (23)$$

where

$$g_n(q) = \varepsilon_p \coth nqa_p + \sqrt{\varepsilon_{\parallel}\varepsilon_{\perp}} \coth \left( \frac{\varepsilon_{\perp}}{\varepsilon_{\parallel}} \right)^{1/2} nqa_f$$

and the "domain wall width"  $\Delta$  can be found by integration of the Landau energy of the wall as  $\Delta = \frac{4\pi}{\varepsilon_{\parallel}} \frac{1}{4} \int_{-\infty}^{\infty} (\tanh^4(x/\sqrt{2}) - 1) dx \approx 8\pi\sqrt{2}/3\varepsilon_{\parallel}$ . This takes into account the fact that  $P(x) = P_0 \tanh(x/\sqrt{2})$  is the exact single-wall solution of Eq. (2) at  $t = -1$ . The result of the numerical minimization of (23) is given by the dashed line in Fig. 2b. When  $qca_p$ ,  $(\varepsilon_{\perp}/\varepsilon_{\parallel})^{1/2} qca_f \gg 1$  it is approximated by the generalized Kittel formula:

$$q_c^2 \approx \frac{\varepsilon_{\parallel}}{\varepsilon_p + \sqrt{\varepsilon_{\parallel}\varepsilon_{\perp}}} \frac{21\zeta(3)}{2\pi\sqrt{2}} \frac{1}{2a_f} \approx 2.8. \quad (24)$$

Since, as shown in Fig. 2, the plots  $q(\Lambda)$  at  $T = 0$  and at  $T = T_c$  practically coincide, we conclude that the temperature dependence of the domain structure wave vector is very weak. The complete calculation of the domain structure evolution and of its dielectric constant over the entire temperature region will be published elsewhere.

To conclude, we have demonstrated that uniaxial ferroelectric domains can substantially influence the properties of the FE/PE superlattices. Depending on the wavelength  $\Lambda$ , the superlattice can be in different domain states. For large  $\Lambda$  (typically  $> 5 - 15nm$ ) each FE layer has an independent domain structure. At smaller  $\Lambda$  the domains in neighboring FE layers interact through the PE layers via the emerging depolarization field and this results in a dramatic increase of the domain width. In this regime the superlattice structure behaves as an effective composite uniform ferroelectric where the large-scale domains penetrate throughout the entire sample and are governed by the global depolarization field.

We have calculated the ferroelectric transition temperature as function of  $\Lambda$  and have explained the recently observed small- $\Lambda$  saturation of  $T_c$  in  $\text{KTaO}_3/\text{KNbO}_3$  superlattice by crossover to the regime of strongly coupled FE layers. We have also shown that the critical superlattice crossover wavelength is nearly temperature independent.

We gratefully acknowledge the Region of Picardy and the European Social Fund for financial support.

- 
- [1] J. F. Scott, *Ferroelectrics Memories* (Springer, 2000)
  - [2] S. Hong, *Nanoscale Phenomena in Ferroelectric Thin Films* (Springer, 2004)
  - [3] H. Ishiwara, M. Okuyama and Y. Arimoto, *Ferroelectric Random Access Memories: Fundamentals and Applications* (Springer, 2004)
  - [4] N. A. Pertsev, A. G. Zembilgotov, and A. K. Tagantsev, *Phys. Rev. Lett.* **80**, 1988 (1998)
  - [5] I. P. Batra and B. D. Silverman, *Sol. St. Commun.* **11**, 291 (1972)
  - [6] A. M. Bratkovsky and A. P. Levanyuk *Phys. Rev. Lett.* **84**, 3177 (2000)
  - [7] A. L. Roitburd, *Phys. Status Solidi* **A37**, 329 (1976)
  - [8] B. S. Kwak et al., *Phys. Rev. Lett.* **68**, 3733 (1992)
  - [9] E. D. Specht, H.-M. Christen, D.P. Norton and L.A. Boatner, *Phys. Rev. Lett.* **80**, 4317 (1998)
  - [10] M. Sepiarsky, S. R. Phillpot, M. R. Stachiotty and R. L. Migoni, *J. Appl. Phys.* **91**, 3165 (2001)
  - [11] C. Kittel, *Phys. Rev.* **70**, 965 (1946)
  - [12] L. D. Landau and E. M. Lifshitz, *Electrodynamics of Continuous Media* (Elsevier, New York, 1985)
  - [13] B. A. Strukov and A. P. Levanyuk, *Ferroelectric Phenomena in Crystals* (Springer, Berlin, 1998)
  - [14] E. V. Chensky and V. V. Tarasenko, *Sov. Phys. JETP* **56**, 618 (1982) [*Zh. Eksp. Teor. Fiz.* **83**, 1089 (1982)]
  - [15] R. Kretschmer and K. Binder *Phys. Rev.* **B20**, 1065 (1979)
  - [16] Y. G. Wang, W. L. Zhong and P. L. Zhang, *Phys. Rev.* **B51**, 5311 (1995)